

PACS numbers: 62.20.-x, 63.20.dk, 71.15.-m, 71.15.Mb, 71.20.Nr, 71.27.+a

## Effect of Atomic Substitutions on the Electronic Structure of $\text{Pt}_{1-x}\text{Me}_x\text{MnSb}$ ( $\text{Me} = \text{Ni}, \text{Cu}; x = 0.0\text{--}1.0$ )

V. M. Uvarov, M. V. Uvarov, and M. V. Nemoshkalenko

*G. V. Kurdyumov Institute for Metal Physics, N.A.S. of Ukraine,  
36 Academician Vernadsky Blvd.,  
UA-03142 Kyiv, Ukraine*

Using band calculations within the FLAPS (full-potential linearized augmented-plane waves) model, information is obtained about the energy, charge, and spin characteristics of  $\text{Pt}_{1-x}\text{Me}_x\text{MnSb}$  alloys ( $\text{Me} = \text{Ni}, \text{Cu}; x = 0.0\text{--}1.0$ ). As established, with an increase in the concentration of the nickel or copper atoms, the interatomic spatial density of electrons decreases, covalent bonds are weakened, and the binding energies of atoms in alloys decrease. As found, the dominant contributions to the formation of magnetic moments are made by 3d electrons of manganese atoms, and the polarization of electrons at Fermi levels is dependent on the composition of alloys.

**Key words:** band-structure calculations, Heusler alloys, band structure, magnetic moments, polarized band structure states, spintronics.

За допомогою зонних розрахунків у моделі FLAPS (the full-potential linearized augmented-plane waves) одержано інформацію про енергетичні, зарядові та спінові характеристики стопів  $\text{Pt}_{1-x}\text{Me}_x\text{MnSb}$  ( $\text{Me} = \text{Ni}, \text{Cu}; x = 0,0\text{--}1,0$ ). Встановлено, що зі збільшенням концентрації атомів Нікелю або Купруму зменшується міжатомова просторова густина електронів, послаблюються ковалентні зв'язки та понижуються енергії зв'язку атомів у стопах. Виявлено, що домінують внески у формування магнетних моментів вносять 3d-електрони атомів Мангану, а поляризація електронів на рівнях Фермі залежить від складу стопів.

**Ключові слова:** зонні розрахунки, Гейслерові стопи, електронна будова,

---

Corresponding author: Viktor Mykolayovych Uvarov  
E-mail: [uvarov@imp.kiev.ua](mailto:uvarov@imp.kiev.ua)

Citation: V. M. Uvarov, M. V. Uvarov, and M. V. Nemoshkalenko, Effect of Atomic Substitutions on the Electronic Structure of  $\text{Pt}_{1-x}\text{Me}_x\text{MnSb}$  ( $\text{Me} = \text{Ni}, \text{Cu}; x = 0.0\text{--}1.0$ ), *Metallofiz. Noveishie Tekhnol.*, 45, No. 4: 443–456 (2023).  
DOI:10.15407/mfint.45.04.0443

магнетні моменти, поляризовані електронні стани, спінтроніка.

(Received 10 February, 2023; in final version, 28 February, 2023)

## 1. INTRODUCTION

A variety of materials with complex crystal structures that exhibit unusual electronic and magnetic properties have always attracted considerable attention from both theorists and experimenters for the purpose of using these unconventional properties in possible practical applications. One such group of materials which is being actively investigated at the moment are the Heusler compounds. The parent Heusler compounds, the so-called the full-Heusler phases ( $L2_1$ -structures), have the general formula  $X_2YZ$ , where  $X$  and  $Y$  are transition metals and  $Z$  is an  $sp$ -valent elements. The half-Heusler phases ( $C1_b$ -structures) have the same structure, except that one of the sites occupied by the  $X$  atom in the parent compound is empty, giving a general formula  $XYZ$  [1]. These phases have [2–5] a complex of magnetic, kinetic, optical, magneto-optical, superconducting, thermoelectric, and other important properties. In the system of compounds under discussion, it is possible to implement topological insulators and the so-called half-metallic state of a solid with a completely uncompensated spin density of band electrons at the Fermi level—an important property necessary in technologies for creating materials for spintronics devices.

In 1983, de Groot and co-workers [6] discovered by ab-initio calculations that one of the half-Heusler alloys, NiMnSb, is half-metallic, *i.e.*, the minority band have a band gap at the Fermi level. This conclusion is confirmed in a series of other works (see, for example, reviews [7, 8]).  $C1_b$ -type Heusler compounds have attracted much attention since the discovery of the very large Kerr effect in PtMnSb [9]. This large effect, a maximum of  $1.3^\circ$  at 1.7 eV in the room-temperature Kerr-rotation spectrum, has been attributed to the unusual electronic structure of this material. Long-standing calculations [6] of the zone structure showed that PtMnSb belongs to the class of so-called half-metallic materials, but there is no convincing experimental evidence for this fact in the literature. Moreover, in the calculations [7, 8], the value of 66.5% was obtained for the polarization of valence electrons at the Fermi level in the PtMnSb compound.

$MeMnSb$  alloys ( $Me = Ni, Pt$ ) are ferromagnets with Curie temperatures, resistive and magnetic characteristics depending on the type of  $Me$  atom [10]. The addition of copper atoms to the MnSb-‘matrix’ preserves the  $C1_b$  structural type of the CuMnSb alloy with its phase transition from the antiferromagnetic to the paramagnetic state at  $T_N \cong 50$  K [10–13]. A fully potential non-orthogonal local-orbital

scheme (FPLO) was used for scalar-relativistic calculations of the paramagnetic phase of CuMnSb in the local density approximation (LDA) [13]. The scalar-relativistic scheme did not allow the authors of the cited work to obtain the most important characteristics of the paramagnetic state of CuMnSb associated with the local magnetic moments of its atoms. The ferromagnetic and antiferromagnetic ordered phases of CuMnSb are calculated here [13] and in [14, 15] using the spin-polarized approach. A common disadvantage of these works is the impossibility of modelling a completely disordered magnetic state of a CuMnSb paramagnet.

An effective way to influence the properties of Geisler phases is the synthesis of solid solutions based on them. Good model systems of this plan are a series of  $\text{Pt}_{1-x}\text{Me}_x\text{MnSb}$  alloys ( $\text{Me} = \text{Ni, Cu}$ ;  $x = 0.0-1.0$ ) [16, 17]. Here, using x-ray diffraction, the parameters of their cubic lattices were determined, as well as magnetic, magneto-optical characteristics, temperatures Curie and temperature dependence of saturation magnetization were measured.

Outside of the cited works, a number of comparative characteristics of the electronic structure of these alloys have not been studied. There was no complete information about their energy characteristics, the spin and charge states of atoms, the nature of interatomic chemical bonds, the structure of valence bands and conduction bands. In addition, the comparative possibilities of spin-independent and spin-polarized band calculations in the correctness of the description of the paramagnetic state of the CuMnSb alloy remain unanalysed.

This paper is devoted to finding answers to these problems.

## 2. THE METHODOLOGY OF THE CALCULATIONS

The ‘parent’ half-Heusler  $\text{MeMnSb}$  ( $\text{Me} = \text{Ni, Cu, Pt}$ ) alloys crystallize in cubic syngony with the space group  $F-43m$  (No. 216) [10, 12]. Experimental studies of alloys of mixed atomic composition  $\text{Pt}_{1-x}\text{Me}_x\text{MnSb}$  alloys ( $\text{Me} = \text{Ni, Cu}$ ;  $x = 0.0-1.0$ ) [16, 17] did not reveal a significant rearrangement of the symmetry of their cubic crystal lattices. To simplify the calculation procedure in this paper, the positions of the component-atoms of the  $\text{Pt}_{1-x}\text{Me}_x\text{MnSb}$  alloys ( $\text{Me} = \text{Ni, Cu}$ ;  $x = 0.0-1.0$ ) are set using the symmetry operations of a simple cubic lattice  $P$ . The correctness of this approach on the example of the study of half-Heusler phases is proved by us in [18, 19].

Band calculations were performed by the LAPW method [20] with a gradient approximation of the electron density (GGA—generalized gradient approximation) in the form [21]. A spin-polarized version of this method was used to calculate the characteristics of the electronic structure [22]. The non-magnetic ( $NM$ ) phase of CuMnSb is calculated in the approximation of a non-spin-polarized version of the Wien2k

software package [22].

The parameters  $a$  of the cubic lattices of the  $\text{Pt}_{1-x}\text{Me}_x\text{MnSb}$  alloys ( $\text{Me} = \text{Ni}, \text{Cu}$ ;  $x = 0.0-1.0$ ) required for the calculations are borrowed from the experimental data, obtained in [16, 17]. The radii ( $R_{\text{mt}}$ ) of the MT (muffin-tin)-atomic spheres were chosen from the consideration of minimizing the size of the intersphere region in the NiMnSb alloy, which has the smallest unit cell volume. For all alloys and all the atoms in them, these radii were 2.18 Bohr radius (1 Bohr radius =  $5.2918 \cdot 10^{-11}$  m). When calculating the characteristics of the electronic structure of all alloys, 172 points in the irreducible parts of their Brillouin zones were used. APW+lo bases are used to approximate the wave functions of the 3d electrons of all atoms, and LAPW bases are used for the wave functions of the remaining valence electrons. The size of the basis set was determined by setting the product  $R_{\text{mt}}K_{\text{max}} = 7.0$  ( $K_{\text{max}}$  is the maximum value of the inverse lattice vector). When selecting the maximum orbital quantum number for partial waves inside the MT spheres, the value  $l = 10$  is used. The non-muffin-tin matrix elements were calculated using  $l = 4$ .

The binding energies ( $E_{\text{coh}}$ —cohesion energies) were calculated as the differences between the total energies of the atoms forming the unit cells of the alloys themselves, and the sum of the total energies of their constituent atoms, separated from each other by ‘infinity’. They were determined in accordance with the recommendations [23].

The degree of polarization ( $P$ ) of Fermi electrons was determined by the formula [24]:

$$P = \frac{D_{\uparrow}(E_F) - D_{\downarrow}(E_F)}{D_{\uparrow}(E_F) + D_{\downarrow}(E_F)},$$

where  $D_{\uparrow}(E_F)$  and  $D_{\downarrow}(E_F)$  are the total electron state densities at the Fermi level ( $E_F$ ) with the spin directions up and down, respectively.

### 3. RESULTS AND DISCUSSION

The concentration dependences of the parameters  $a(x)$  of the crystal lattices of alloys correlate with their binding energies and electron densities in the interatomic region (Fig. 1). The declining trend of curve  $a(x)$  with an increase in nickel concentrations in  $\text{Pt}_{1-x}\text{Ni}_x\text{MnSb}$  alloys ( $x = 0.0-1.0$ ) is due to a reduced atomic radius of nickel 1.24 Å compared to the same for platinum atoms, equal to 1.39 Å [27]. As a consequence of this and the already mentioned ‘striving’ of alloys for dense atomic packages ( $F$ -structures) this inevitably leads to a decrease in the values of parameter  $a$  with an increase in the nickel concentration in the alloys. If the atomic radii of the substituting components exceed the size of the platinum atoms, then, according to the above

considerations, in a series of solid solutions, the parameter  $a$  should increase with increasing concentrations of the embedded atoms. Indeed, such a pattern can be seen [17] for a series of  $\text{Pt}_{1-x}\text{Au}_x\text{MnSb}$  ( $x = 0.0-1.0$ ) alloys, for which the atomic radius of gold is  $1.44 \text{ \AA}$  [27]. Another confirmation of the above assumptions is the course of the dependence  $a(x)$  in  $\text{Pt}_{1-x}\text{Cu}_x\text{MnSb}$  ( $x = 0.0-1.0$ ) series alloys: here (Fig. 1), at an atomic radius of  $1.28 \text{ \AA}$  copper [27], a decreasing course of the curve  $a(x)$  at  $x \rightarrow 1.0$  is observed, as in nickel alloys. It should be noted that the current values of  $a(x)$  in copper alloys exceed those for nickel alloys. The latter circumstance is explained by the somewhat larger radius of the copper atoms.

In the works [18, 19, 25], it was found that the chemical composition and atomic disordering affect the interatomic bond energies, the degree of their covalence, and the parameters of the unit cells in half-Heusler alloys. Similar dependences, as indicated in Fig. 1, are also characteristic of  $\text{Pt}_{1-x}\text{Me}_x\text{MnSb}$  ( $\text{Me} = \text{Ni, Cu}$ ;  $x = 0.0-1.0$ ) alloys. The drop in the charge density in the interatomic region is accompanied by a decrease in the binding energies of the atoms in the alloys under study. Based on this and the valence theory [26], the following conclusion can be formulated: a decrease in the spatial density of electrons in interatomic regions with an increase in the concentration of nickel or

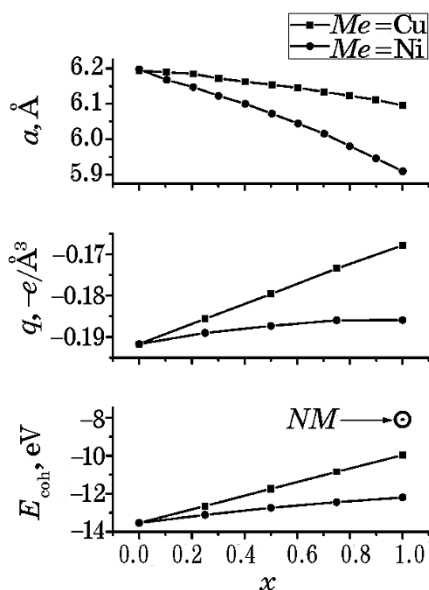


**Fig. 1.** Concentration dependences of parameters ( $a$ ) [17] of conventional cells, electron densities ( $q$ ,  $e$ -electron charge) in the interatomic regions and atomic binding energies ( $E_{\text{coh}}$ ) of  $\text{Pt}_{1-x}\text{Me}_x\text{MnSb}$  alloys.  $NM$ — $E_{\text{coh}}$  of non-magnetic phase  $\text{CuMnSb}$ .

copper atoms in  $\text{Pt}_{1-x}\text{Me}_x\text{MnSb}$  ( $\text{Me} = \text{Ni}, \text{Cu}; x = 0.0-1.0$ ) alloys leads to a weakening of covalent chemical interatomic bonds. This fact may indicate a possible loss of thermodynamic stability of alloys with an increase in the concentrations of substitution atoms in them. This instability is most characteristic of alloys with copper, since their binding energies are lower in comparison with those for phases with nickel.

As can be seen from the figure discussed, the binding energy of atoms in the  $\text{CuMnSb}$  alloy obtained in the spin-polarized version of the calculation exceeds such for the non-magnetic state. The difference between the corresponding  $E_{\text{coh}}$  values reaches 1.867 eV. This may indicate that the spin-polarized version of the calculations more correctly describes the electronic structure of the  $\text{CuMnSb}$  alloy.

In Figure 2, it can be seen that with increasing nickel concentration in  $\text{Pt}_{1-x}\text{Ni}_x\text{MnSb}$  alloys, the number of electrons in atomic spheres increases monotonically. Note that the transition to alloys with a maximum nickel concentration is accompanied by an increase in the number of electrons on the Pt, Sb, Ni and Mn atoms by 0.09, 0.06, 0.41 and 0.12 percent, respectively. In alloys with copper, the transition to alloys with its maximum concentration is accompanied by an increase in the number of electrons in the spheres of Pt, Sb and Cu atoms by 0.04,

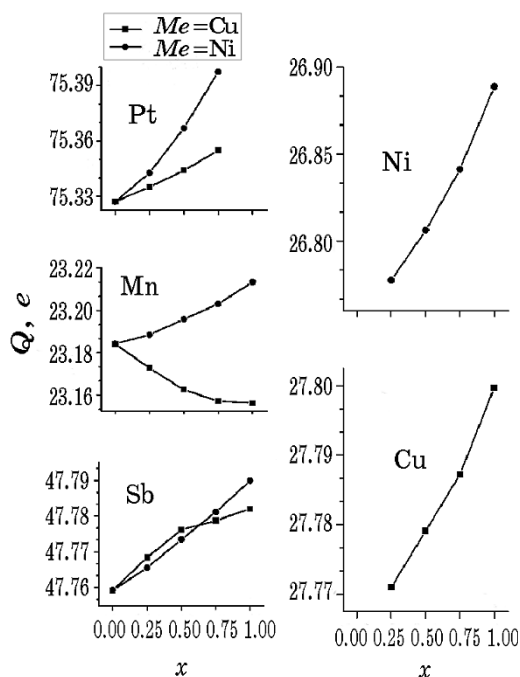


Fig. 2. Concentration dependences of atomic charges ( $Q$ ,  $e$ —electron charge) of  $\text{Pt}_{1-x}\text{Me}_x\text{MnSb}$  alloys.

0.05 and 0.1 percent, respectively. The charges of manganese atoms decrease by 0.13% when the concentrations of copper atoms change to their maximum values.

As can be seen, the changes in  $Q$  values for Sb and Pt atoms are insignificant, whereas for 3*d*-metal atoms the  $Q$  changes turn out to be much higher. A possible reason for such variations in  $Q$  is an increase in the degree of delocalization of valence electrons in a number of Pt, Sb, Ni, Mn atoms—a reaction to a sequential decrease in the charges of the nuclei of these elements. In particular, the increased delocalization of valence electrons of nickel and manganese atoms provides increased dynamics of the formation of their chemical bonds with surrounding atoms and, as a consequence, leads to large changes in  $Q$  values. Note also that the values of charges on the same type of atoms in the composition of alloys with nickel exceed those in alloys with copper. Undoubtedly, this is due to the lower values of the parameters  $a$  of the crystal lattices of nickel alloys (Fig. 1).

Additional information about the nature of chemical bonds in the studied alloys can be obtained by considering the energy structure of their valence bands and zones of vacant states. The corresponding data in the form of curves representing the electron state densities are shown in Fig. 3, 4.

The total densities and total atomic densities of the electronic states of the studied phases for both spin orientations are complex structures that vary depending on the atomic composition of the alloys. It can be seen from the discussed figures that the influence of the atomic composition of alloys manifests itself in a change in the shape and energy localization of the densities of electronic states.

The maximum contributions to the densities of states from antimony atoms in all alloys are concentrated in the region of deep lying ( $\cong -10$  eV) quasi-core states genetically associated with Sb5*s*-electrons. In general, these contributions are insignificant. The states of antimony atoms in the region of valence electron localization (0–5 eV) have even smaller contributions. This indicates that the antimony atoms in the crystal lattices of the alloys are mainly held by ionic bonds.

The localization of the electronic states of metal atoms in this energy region and their hybridization indicate that the metal atoms in the alloys are bound together mainly by covalent interaction. Their further analysis is based on the basic principles of quantum chemistry [26]: in the absence of spatial symmetry constraints, the degree of interactions of the electrons entering into chemical bonds depends on the proximity of their energies and manifests itself in the energy splitting of the final states and the degree of their hybridization.

As can be seen from Fig. 3, these characteristics of the electronic states of metal atoms depend on the atomic composition of the alloys. In the PtMnSb alloy, the states of metal atoms occupy close energy po-

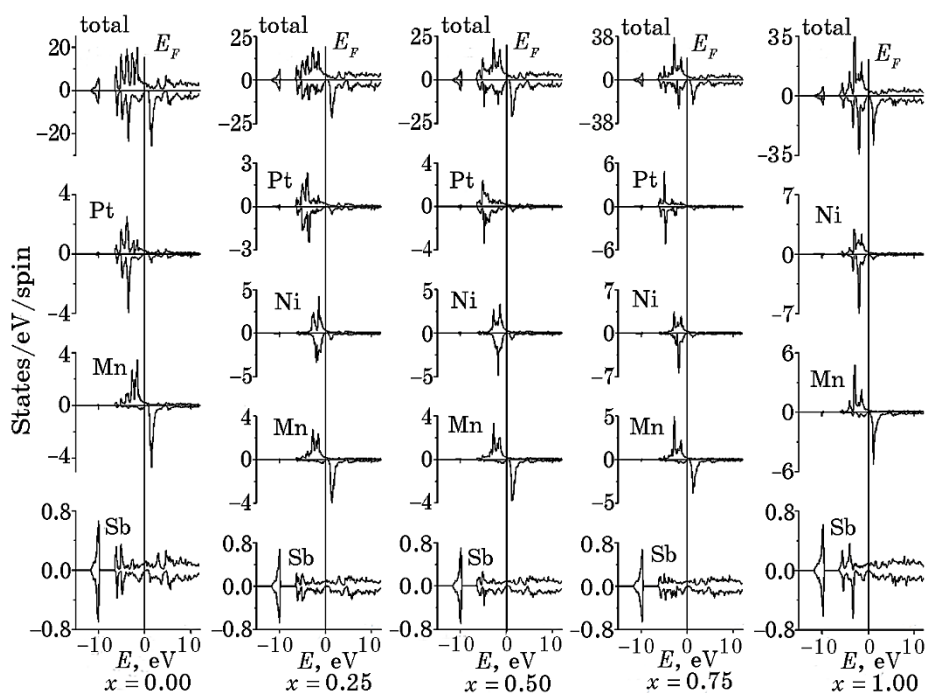


**Fig. 3.** Total electron densities (top panel) and total atomic electron densities of  $\text{Pt}_{1-x}\text{Ni}_x\text{MnSb}$  alloys ( $x = 0.0\text{--}1.0$ ). Densities with positive and negative values correspond to the spin-up and spin-down orientations of the electrons respectively.  $E_F$  is the position of the Fermi level.

sitions, hybridize well, and split energetically. These facts indicate a high degree of covalence of Pt–Mn chemical bonds, which provides high values of the binding energy of the PtMnSb alloy (Fig. 1).

A consistent increase in the nickel concentration in  $\text{Pt}_{1-x}\text{Ni}_x\text{MnSb}$  alloys ( $x = 0.0\text{--}1.0$ ) is accompanied by a decrease in the degree of hybridization of the electronic states of platinum atoms. In the limiting case ( $x = 0.75$ ), the electronic states of platinum turn out to be localized in a narrow energy region remote from those similar for nickel and manganese atoms. The latter remain split and hybridized when the nickel concentration changes, thereby providing covalent Mn–Ni interactions. Based on these arguments, we can understand the fact that the decrease in the binding energy (Fig. 1) of  $\text{Pt}_{1-x}\text{Ni}_x\text{MnSb}$  alloys ( $x = 0.0\text{--}1.0$ ) alloys is probably due to a decrease in covalent interactions of platinum atoms with surrounding atoms.

It also follows from Fig. 3 that the states of the conductivity bands of the alloys are mainly formed by the electrons of the manganese atoms with a spin-down orientation. Attention is drawn to the discrepancy between the shapes and values of the electron densities correspond-



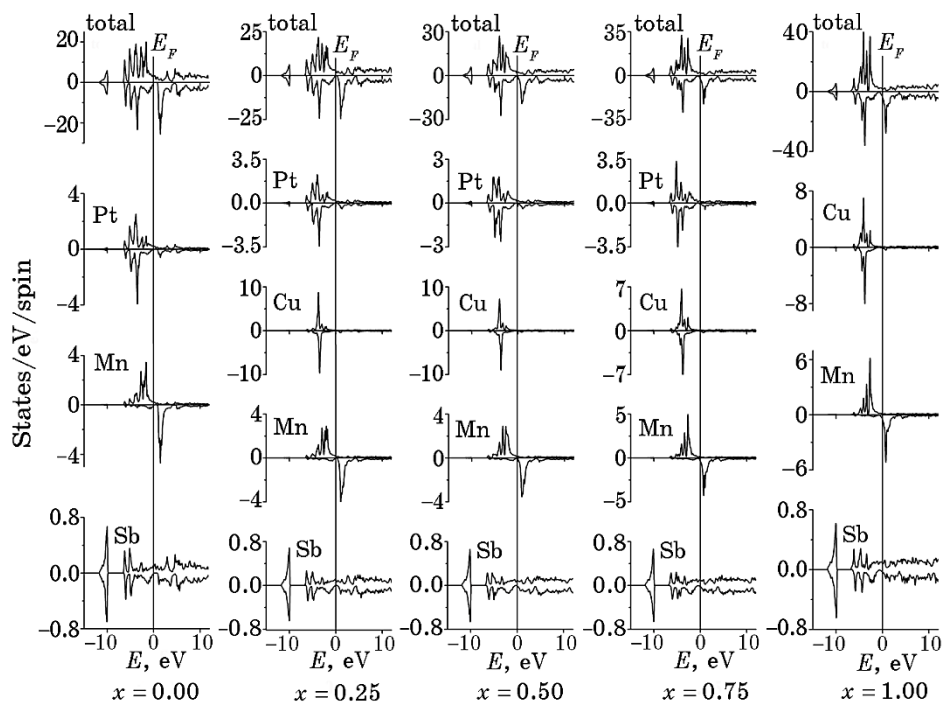


**Fig. 4.** Total electron densities (top panel) and total atomic electron densities of  $\text{Pt}_{1-x}\text{Cu}_x\text{MnSb}$  alloys ( $x = 0.0-1.0$ ). Densities with positive and negative values correspond to the spin-up and spin-down orientations of the electrons respectively.  $E_F$  is the position of the Fermi level.

ing to different spin directions, which indicates the polarization of the electronic states. This effect is most pronounced in manganese.

A similar pattern is observed (Fig. 4) for hybridized states of atoms in alloys with copper. Here, an increase in copper concentrations in alloys has a noticeable effect on the hybridization of the states of platinum and manganese atoms, while the states of copper atoms turn out to be energetically more localized and less split. All these ones lead to such changes in interatomic chemical bonds that with increasing concentrations of copper, the cohesion energies of alloys fall (Fig. 1). The qualitative conclusions obtained for the structure of the conduction band are fully characteristic of alloys with copper. This follows from a comparison of the distributions of electronic states shown in Fig. 3 and Fig. 4.

There was also a discrepancy between the shapes and values of electron densities corresponding to different spin directions, which indicates the polarization of electronic states. As in nickel alloys, this effect was most pronounced for the electronic states of manganese at-

oms.

Polarization effects lead to the appearance of magnetic moments on atoms. It is useful to consider the question to what extent certain electronic states are involved in the formation of magnetic moments on the atoms of the alloys under discussion? The corresponding data are shown in Fig. 5. The determining contribution to the formation of magnetic moments in alloys is associated with the  $3d$  electrons of manganese atoms. The contribution of Mn  $s$ ,  $p$ -electrons is insignificant. This can be completely attributed to the electrons of all symmetries of atoms of other metals and antimony in all types of alloys.

Figure 6 shows the concentration dependences of magnetic moments and electron polarizabilities in  $\text{Pt}_{1-x}\text{Me}_x\text{MnSb}$  alloys ( $\text{Me} = \text{Ni}, \text{Cu}; x = 0.0-1.0$ ). In the experimental work [16] it was noted that the values of these magnetic moments essentially remain constant over the entire range of nickel concentrations in alloys. In Figure 6, this is indicated by a horizontal line, which, according to the authors, is the result of averaging experimental data. These data at the qualitative level coincide with those obtained in this work. Indeed, the calculated values of the magnetic moments practically do not depend on the concentration

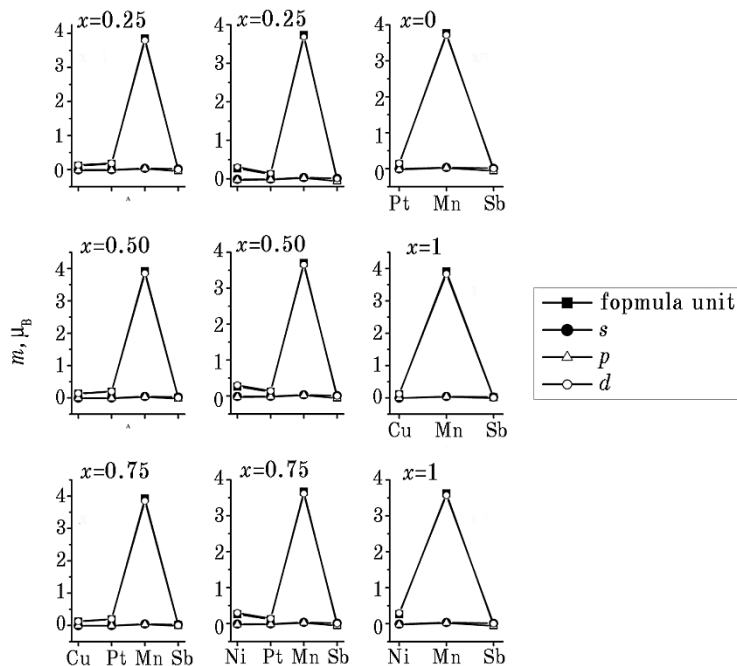


**Fig. 5.** Partial contribution of electronic states to the formation of magnetic moments ( $m$ ,  $\mu_B$ —Boron magneton) on atoms in  $\text{Pt}_{1-x}\text{Me}_x\text{MnSb}$  alloys ( $\text{Me} = \text{Ni}, \text{Cu}; x = 0.0-1.0$ ).

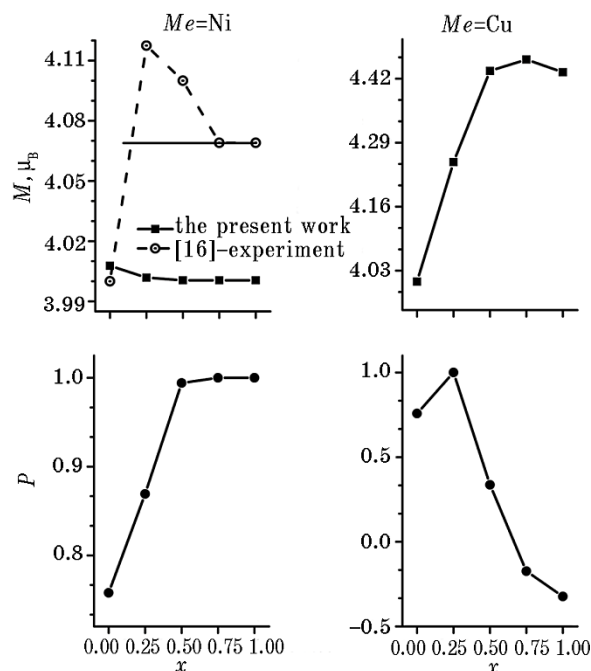


**Fig. 6.** Magnetic moments ( $M$ ) per formula unit of  $\text{Pt}_{1-x}\text{Me}_x\text{MnSb}$  alloys ( $x = 0.0-1.0$ ). The horizontal solid line in the experimental part of the figure is the result of averaging the measurements [16].  $P$ -electron polarization at the Fermi level in  $\text{Pt}_{1-x}\text{Me}_x\text{MnSb}$  alloys.

of nickel atoms in the studied alloys. Recall that the ‘outliers’ of the values of experimentally measured magnetic moments at the content of nickel atoms  $x = 0.25$  in alloys are associated [16] with the presence of other phases with concentrations reaching 15%. In general, the samples studied here also contained other phases in concentrations up to 5%. Perhaps these reasons led to systematic differences between the experimental and calculated values of magnetic moments. Note that these differences for most alloys ( $x \geq 0.25$ ) were of  $\cong 1.5\%$ . As for the initial composition of  $\text{PtMnSb}$ , the experimental and calculated values of the magnetic moments actually coincided.

Substituting nickel atoms change the polarization  $P$  of electrons at the Fermi level (Fig. 6). The transition from the  $\text{PtMnSb}$  metal alloy with a relatively high ( $P = 0.76$ ) electron polarization to alloys with  $x \geq 0.5$  is accompanied by full polarization of Fermi electrons ( $P = 1.0$ ) and converts these alloys to half-metallic state.

Figure 6 also shows that an increase in the concentrations of copper atoms in  $\text{Pt}_{1-x}\text{Cu}_x\text{MnSb}$  alloys increases their magnetic moments up to concentrations  $x = 0.75$ . Then there is a decrease in the values of mag-

netic moments. Note that similar changes in the values of magnetic moments were recorded [28] for similar alloys with  $\text{Pt}_{1-x}\text{Au}_x\text{MnSb}$  gold. In Ref. [17], for a copper alloy with a concentration of  $x = 0.3$ , the maximum value of  $4.4 \mu_B$  of the magnetic moment on Mn atoms was determined by extrapolating experimental data to zero Kelvin temperatures.

In this work, the maximum magnetic moment on manganese atoms was fixed for the  $\text{Pt}_{0.25}\text{Cu}_{0.75}\text{MnSb}$  alloy and amounted to  $3.93 \mu_B$ . The difference of  $\cong 10\%$  of this value from the experimentally determined one may be due to the procedure of inaccurate experimental determination ( $T = 0 \text{ K}$ ) of the values of the magnetic moments under discussion. In addition, we draw attention to the fact that, within the framework of the accepted model (see calculation methodology), the alloy  $\text{Pt}_{0.7}\text{Cu}_{0.3}\text{MnSb}$  is not possible to calculate.

The existence of a ferromagnetically ordered phase in the CuMnSb alloy is possible [12] at temperatures below  $\cong 107 \text{ K}$ . For this reason, and in the presence of structural data obtained at temperatures below the specified temperature, calculations of the electronic structure of the CuMnSb alloy in the band spin-polarized approach receive their justification.

Substituting copper atoms change the polarization of  $P$ -electrons at the Fermi level (Fig. 6). The transition from a PtMnSb metal alloy with a relatively high degree of electron polarization ( $P = 0.76$ ) to an alloy with  $x = 0.25$  is accompanied by complete polarization of Fermi electrons ( $P = 1.0$ ) and converts this alloy to a half-metallic state. A further increase in the content of copper atoms in alloys with  $x \geq 0.5$  translates them into a state of metallic conductivity.

#### 4. CONCLUSIONS

1. The course of the concentration dependences of the parameters  $a(x)$  of cubic crystal lattices of  $\text{Pt}_{1-x}\text{Me}_x\text{MnSb}$  solid solutions ( $\text{Me} = \text{Ni}, \text{Cu}, \text{Au}; x = 0.0-1.0$ ) is determined by the ratio of the radii of the substitution atoms and platinum. If this ratio is less than one ( $\text{Me} = \text{Ni}, \text{Cu}$ ), then the dependence  $a(x)$  ( $x \rightarrow 1.0$ ) has a descending and in the opposite case ( $\text{Me} = \text{Au}$ ) an increasing character.

2. With an increase in the concentration of nickel or copper atoms in  $\text{Pt}_{1-x}\text{Me}_x\text{MnSb}$  alloys ( $\text{Me} = \text{Ni}, \text{Cu}; x = 0.0-1.0$ ), the interatomic spatial density of electrons decreases, which leads to a weakening of interatomic covalent bonds and, consequently, to a decrease in the binding energies of the alloys. These energies for copper alloys are lower compared to those for nickel phases.

3. The densities of the electronic states of  $\text{Pt}_{1-x}\text{Me}_x\text{MnSb}$  ( $\text{Me} = \text{Ni}, \text{Cu}; x = 0.0-1.0$ ) alloys are complex structures that vary in shape, energy position and localization. The zones of valence electrons ( $0--5 \text{ eV}$ ) of

alloys are dominated by hybridized states of metals, while the vacant states are formed mainly by Mn-electrons with spins oriented downwards.

4. Antimony atoms in the crystal lattices of  $\text{Pt}_{1-x}\text{Me}_x\text{MnSb}$  ( $\text{Me} = \text{Ni}, \text{Cu}; x = 0.0-1.0$ ) alloys are mainly held by ionic bonds, whereas metal atoms are mainly covalently bound to each other. Covalent interactions are maximal in PtMnSb and with an increase in the concentration of nickel or copper in alloys they weaken due to a decrease in the role of platinum valence electrons in the formation of chemical bonds.

5. The densities of electronic states with different spin orientations do not correspond to each other that indicates the polarization of electrons in  $\text{Pt}_{1-x}\text{Me}_x\text{MnSb}$  alloys. Polarization effects lead to the appearance of magnetic moments on the atoms. The determining contributions to the formation of magnetic moments in alloys are associated with the  $3d$ -electrons of manganese atoms. The values of the magnetic moments practically do not depend on the concentration of nickel atoms in the studied alloys. An increase in the concentration of copper atoms in  $\text{Pt}_{1-x}\text{Cu}_x\text{MnSb}$  ( $x = 0.0-1.0$ ) alloys leads to an increase in their magnetic moments up to concentrations with  $x = 0.75$ , and then, there is a decrease in the values of magnetic moments.

6. Substituting nickel or copper atoms change the polarization of electrons at the Fermi level of  $\text{Pt}_{1-x}\text{Me}_x\text{MnSb}$  ( $\text{Me} = \text{Ni}, \text{Cu}; x = 0.0-1.0$ ) alloys. The transition from the PtMnSb metal alloy with relatively high ( $P = 0.76$ ) electron polarization to alloys with a nickel concentration of  $x \geq 0.5$  is accompanied by complete polarization ( $P = 1.0$ ) of Fermi electrons and converts these alloys to a half-metallic state. The  $\text{Pt}_{0.75}\text{Cu}_{0.25}\text{MnSb}$  alloy is also a half-metal, and beyond this concentration, alloys with copper are metals.

## REFERENCES

1. G. E. Bacon and J. S. Plant, *J. Phys. F: Metal Phys.*, **1**: 524 (1971).
2. T. Graf, C. Felser, and Stuart S. P. Parkin, *Progress in Solid State Chemistry*, **39**: 1 (2011).
3. I. Galanakis, P. H. Dederichs, and N. Papanikolaou, *arXiv: cond-mat/0203534v3*, 19 Jul 2002, p. 1.
4. C. Felser, G. H. Fecher, and B. Balke, *Angew. Chem. Int. Ed.*, **46**: 668 (2007).
5. I. Galanakis and P. H. Dederichs, *Lect. Notes Phys.*, **676**: 1 (2005).
6. R. A. de Groot, F. M. Mueller, P. G. van Engen, and K. H. J. Buschow, *Phys.Rev.Lett.*, **50**, No. 25: 2024 (1983).
7. I. Galanakis, Ph. Mavropoulos, and P. H. Dederichs, *arXiv: cond-mat/0510276v1*, 11 Oct 2005, p.1.
8. I. Galanakis and Ph. Mavropoulos, *J. Phys.: Condens. Matter*, **19**: 1 (2007).
9. P. G. van Engen, K. H. J. Buschow, R. Jongebreur and M. Erman, *Appl. Phys. Lett.*, **42**: 202 (1983).
10. M. J. Otto, R. A. M. van Woerden, P. J. van der Valk, and J. Wijngaard,

- J. Phys.: Condens. Matter*, **1**: 2341 (1989).
11. K. Endo, *J. Phys. Soc. Japan*, **29**, No. 3, 643 (1970).
  12. Madhumita Halder, S. M. Yusuf, Amit Kumar, A. K. Nigam, and L. Keller, *Phys. Rev. B*, **74**, 024428 (2006).
  13. T. Jeong, Ruben Weht, and W. E. Pickett, *Phys. Rev. B*, **71**, 184103 (2005).
  14. J. Kudrnovský, V. Drchal, I. Turek, and P. Weinberger, *Phys. Rev. B*, **78**: 054441 (2008).
  15. I. Galanakis, E. Şaşıoğlu, and K. Özdoğan, *Phys. Rev. B*, **77**: 214417 (2008).
  16. P. P. J. van Engelen, D. B. de Mooij, J. H. Wijngaard, and K. H. J. Buschow, *J. Magn. Magn. Mater.*, **130**: 247 (1994).
  17. H. Masumoto and K. Watanabe, *Trans. JIM*, **17**: 588 (1976).
  18. V. N. Uvarov, N. V. Uvarov, and S. A. Bespalov, *Metallofiz. Noveishie Tekhnol.*, **38**, No. 3: 305 (2016).
  19. V. N. Uvarov, N. V. Uvarov, S. A. Bespalov, and M. V. Nemoshkalenko, *Ukr. J. Phys.*, **62**, No. 2: 106 (2017).
  20. D. Singh, *Plane Waves, Pseudopotentials and LAPW Method* (Kluwer Academic: 1994).
  21. J. P. Perdew, S. Burke, and M. Ernzerhof, *Phys. Rev. Lett.*, **77**: 3865 (1996).
  22. P. Blaha, K. Schwarz, G. K. Madsen, D. Kvasnicka, J. Luitz, R. Laskowski, F. Tran, and Laurence D. Marks, *WIEN2k, An Augmented Plane Wave + Local Orbitals Program for Calculating Crystal Properties* (Wien, Austria: Techn. Universität: 2001).
  23. [http://www.wien2k.at/reg\\_user/faq/](http://www.wien2k.at/reg_user/faq/)
  24. B. R. K. Nanda and I. Dasgupta, *J. Phys.: Condens. Matter*, **15**: 7307(2003).
  25. V. N. Uvarov and N. V. Uvarov, *Metallofiz. Noveishie Tekhnol.*, **39**, No. 3: 309 (2017).
  26. J. Murrel, S. Kettle, and J. Tedder, *Teoriya Valentnosti* (Moskva: Mir: 1968) (Russian translation).
  27. B. L. Aleksandrov and M. B. Rodchenko, *Patent RF RU2273058C1*, 27.03.2006, Bull.9.
  28. V. N. Uvarov, N. V. Uvarov, and S. A. Bespalov, *Metallofiz. Noveishie Tekhnol.*, **43**, No. 6: 831 (2021).